

EgoSurgery-Tool: A Dataset of Surgical Tool and Hand Detection from Egocentric Open Surgery Videos

Ryo Fujii¹, Hideo Saito¹ and Hiroki Kajita²
¹Keio University, ²Keio University School of Medicine
 {ryo.fujii0112, hs, jmrbox767}@keio.jp

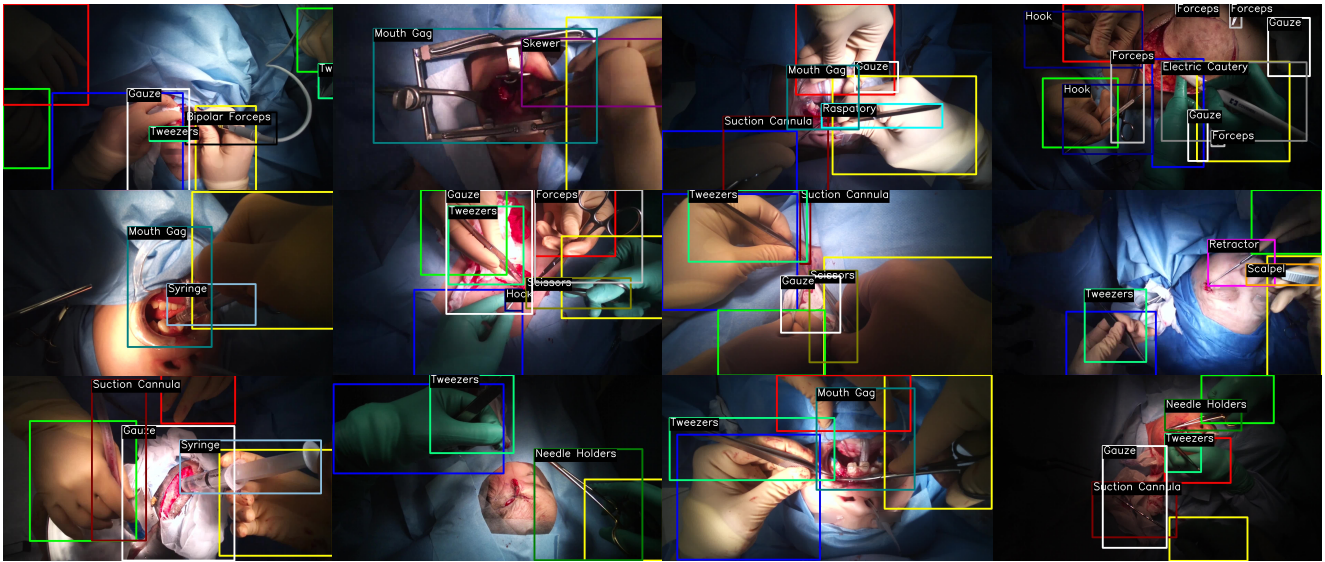


Figure 1. Visualizations of EgoSurgery-Tool and ground truth annotations, for surgical tools, own left hand, own right hand, other left hands, and other right hands.

Abstract

Surgical tool detection is a fundamental task for understanding egocentric open surgery videos. However, detecting surgical tools presents significant challenges due to their highly imbalanced class distribution, similar shapes and similar textures, and heavy occlusion. The lack of a comprehensive large-scale dataset compounds these challenges. In this paper, we introduce EgoSurgery-Tool, an extension of the existing EgoSurgery-Phase dataset, which contains real open surgery videos captured using an egocentric camera attached to the surgeon’s head, along with phase annotations. EgoSurgery-Tool has been densely annotated with surgical tools and comprises over 49K surgical tool bounding boxes across 15 categories, constituting a large-scale surgical tool detection dataset. EgoSurgery-Tool also provides annotations for hand detection with over 46K hand-bounding boxes, capturing hand-object interactions that are crucial for understanding activities in ego-

centric open surgery. EgoSurgery-Tool is superior to existing datasets due to its larger scale, greater variety of surgical tools, more annotations, and denser scenes. We conduct a comprehensive analysis of EgoSurgery-Tool using nine popular object detectors to assess their effectiveness in both surgical tool and hand detection. The dataset will be released at <https://github.com/Fujiry0/EgoSurgery>.

1. Introduction

Detecting surgical tools from an egocentric perspective in the operating room is fundamental task for the development of intelligent systems that can assist surgeons in real-time. For example, recognizing a tool can help prevent accidents, such as leaving gauze inside the body, by notifying surgeons. Recently, various approaches have been proposed for surgical tool detection, particularly in mini-

Table 1. Comparisons of EgoSurgery-Tool and existing datasets for surgical tool detection. *OS* indicates open surgery.

Dataset	Surgery type	Frames	Tool instances	Hand instances	Tool categories	Hand categories	Tool Instances per frame
m2cai16-tool-locations [10]	MIS	2.8K	3.9K		7		1.4
Cholec80-locations [17]	MIS	4.0K	6.5K		7		1.6
AVOS dataset [6]	OS	3.3K	2.8K	6.2K	3	1	0.9
EgoSurgery-Tool (Ours)	OS	15.4K	49.7K	46.3K	15	4	3.2

mally invasive surgeries (MIS) [1, 8, 10, 15, 17, 19, 26]. However, there have been few attempts to detect surgical tools in open surgery videos due to the limited availability of large-scale datasets. The existing surgical tool detection datasets for open surgery are either small [6] or not publicly available [7]. In contrast, several datasets [10, 13, 17] have been released for MIS, driving advancements in learning-based algorithms. The absence of comparable large-scale datasets for open surgical tool detection has significantly impeded progress in achieving accurate tool detection within the open surgery domain. Challenges include dealing with surgical tools that exhibit a highly imbalanced, long-tailed distribution, have similar textures and shapes, and appear in occluded scenes, posing new challenges for many existing approaches.

Hand detection is an essential task for egocentric video analysis, where hand-object interaction (HOI) is crucial for action localization and understanding in activities of daily living. Several large-scale hand detection datasets have been proposed [2, 3, 16] for detecting hands in daily activities. Localizing hands is also vital for analyzing egocentric open surgery videos. However, there is little work on hand detection in the open surgery domain [6, 21], and only one small publicly available dataset exists [6]. Training on existing hand datasets from daily activities does not transfer well to surgical hand detection due to significant differences in domain appearance, highlighting the need for a large-scale dataset.

With these motivations, we introduce EgoSurgery-Tool, a large-scale dataset captured from a camera attached to the surgeon’s head, containing dense annotations for surgical tools and the surgeon’s hand-bounding boxes. EgoSurgery-Tool is an extension of the recently introduced EgoSurgery-Phase [9]. We now elaborate on the unique characteristics and differences between the existing dataset [6] and our proposed EgoSurgery-Tool dataset. Compared to the existing dataset [6], EgoSurgery-Tool offers several advantages: 1) it is the largest-scale dataset among tool and hand detection datasets in the open surgery domain in terms of the number of images and annotations; 2) it contains a greater variety of surgical tools; 3) it includes high-density scenes with numerous surgical tools; and 4) each hand annotation specifies hand identification (the camera wearer’s left or right

Table 2. Comparison of datasets with respect to image distribution across various instance count ranges. We compute the number of images for each dataset within three count ranges.

Datasets	# Image (0-5 instances)	# Image (6-10 instances)	# Image (11-15 instances)
m2cai16-tool-locations [10]	2,811	0	0
EgoSurgery-Tool	6,128	8,803	506

hand or another person’s left or right hand). Our dataset is compared with existing related datasets in Table 1, and example images are shown in Figure 1. Based on the proposed EgoSurgery-Tool dataset, we provide a systematic study on nine mainstream baselines.

2. EgoSurgery-Tool Dataset

The EgoSurgery-Phase dataset [9] consists of 21 videos covering 10 distinct surgical procedures, with a total duration of 15 hours, performed by 8 surgeons. EgoSurgery-Phase provides over 27K frames with phase annotations. However, EgoSurgery-Phase lacks sufficient information on surgical tools and hands. Therefore, we propose EgoSurgery-Tool, which includes additional annotations for surgical tools and hands on a subset of the existing EgoSurgery-Phase dataset. These annotations make EgoSurgery-Phase the only available dataset for multi-task learning of phase recognition, surgical tool detection, and hand detection. EgoSurgery-Phase is manually annotated by a group of annotators who were instructed for each task to ensure consistency across the dataset. The annotations were then inspected by expert surgeons to assess their quality. The rest of this section provides details on the annotations, benchmarking, and statistics of EgoSurgery-Tool.

2.1. Data splits and statistic

We annotated 15 types of surgical tools and 4 types of hands in 15 videos from the EgoSurgery-Phase dataset. The proposed EgoSurgery-Tool dataset contains 15,437 high-quality images, annotated with 49,652 surgical tools and 46,320 hands. The distribution of surgical tools, shown in Figure 2, reveals a notable class imbalance. Figure 3 shows The distribution of hand. Table 2 shows the number of im-

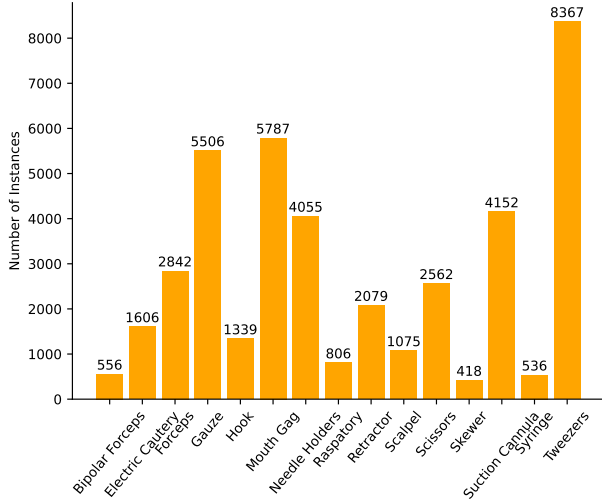


Figure 2. The distribution of surgical tool categories.

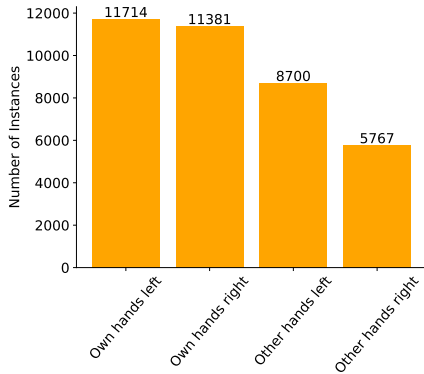


Figure 3. The distribution of hand categories.

ages within each instance count range (0-5, 6-10, 11-15). Our EgoSurgery-Phase dataset demonstrates higher density compared to the surgical tool detection dataset in MIS. The co-occurrence matrix between surgical tools and surgical phases is presented in Figure 4. Along the Y-axis are the given surgical tools, and the X-axis enumerates conditional phases. Each element represents the conditional probability that a phase occurs when a surgical tool is used. For example, when a scalpel appears in a frame, that frame belongs to the incision phase with a probability of 0.98. Surgical tool information might be helpful for surgical phase recognition. EgoSurgery-Tool is divided into training, validation, and test sets at the video level, ensuring that all frames of a video sequence appear in one specific split. The 15 video sequences are split into 10 training, 2 validation, and 3 test videos for consistency with the standard evaluation of other relevant datasets, resulting in 9,657 training, 1,515 validation, and 4,265 test images. The number of instances per category in each set is shown in Table 3.

Table 3. The number of instances per category in each set and the category distribution in the EgoSurgery-Tool dataset.

(a) The number of instances per surgical tool category.

Class	Train	Val	Test	Total	Dist.
Bipolar Forceps	446	55	195	696	1.40%
Electric Cautery	1,404	101	162	1,667	3.36%
Forceps	2,534	154	3,375	6,063	1.22%
Gauze	4,596	455	1,644	6,695	13.58%
Hook	1,045	147	157	1,349	2.72%
Mouth Gag	3,807	990	1,188	5,985	12.05%
Needle Holders	3,031	512	1,286	4,829	9.73%
Raspatory	654	76	84	814	1.64%
Retractor	2,079	0	325	2,404	4.84%
Scalpel	739	168	159	1,066	2.15%
Scissors	1,780	391	565	2,736	5.51%
Skewer	212	103	29	344	0.69%
Suction Cannula	3,134	509	768	4,411	8.88%
Syringe	344	96	141	581	1.17%
Tweezers	6,467	950	2,595	10,012	20.16%
Total	32,272	4,707	12,673	49,652	100%

(b) The number of instances per hand category.

Class	Train	Val	Test	Total	Dist.
Own hands left	8,704	1,505	3,834	14,043	30.3%
Own hands right	8,447	1,467	3,670	13,584	29.3%
Other hands left	6,542	1,079	3,412	11,033	29.3%
Other hands right	4,033	867	2,760	7,660	16.5%
Total	27,726	4,918	13,676	46,320	100%

3. Experiments

3.1. Experimental setups

We compare nine popular object detectors: Faster R-CNN (2015) [14], RetinaNet (2017) [11], Cascade R-CNN (2018) [4], CenterNet (2019) [24], Sparse R-CNN (2021) [18], VarifocalNet (2021) [23], Deformable-DETER (2021) [25], DDQ (2023) [22], and DINO (2023) [20]. We use the MMDetection [5] for the implementation. We fine-tune models with pre-trained on MS-COCO [12]. For a fair comparison, we select the algorithm’s backbones to have a similar number of parameters. We use the COCO evaluation procedure and report AP , AP_{50} , and AP_{75} [12]. Because each detector is calibrated differently, setting a comparable detection confidence threshold is impractical. Therefore, we evaluate all the detectors by using confidence 10^{-8} .

3.2. Quantitative results

We present the results of nine mainstream object detection algorithms in Table 4. For surgical tool detection, among all methods, the recent VarifocalNet achieves the highest performance in terms of the AP metric for surgical tool detection tasks. VarifocalNet also consistently out-

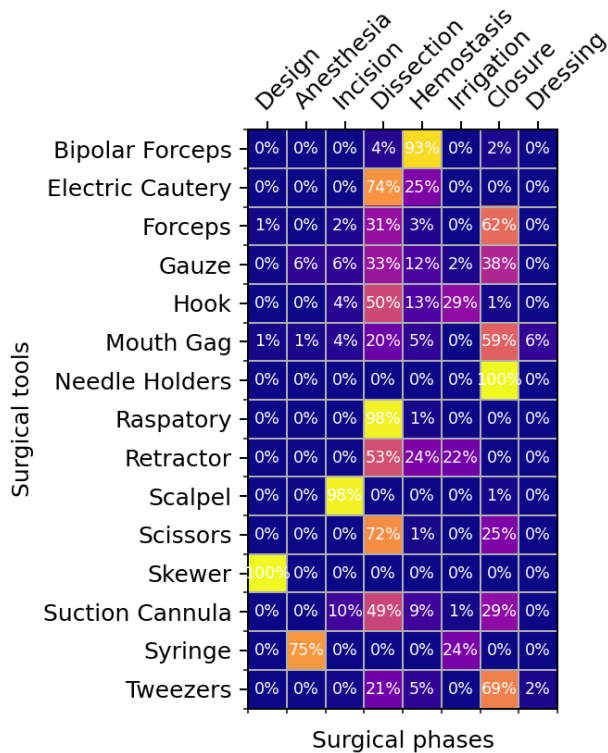


Figure 4. Co-occurrence matrix between surgical tools and surgical phases.

performs other detectors in terms of AP_{75} and AP_{50} , indicating its superior ability to estimate the correct bounding box sizes. The superiority of VarifocalNet is attributed to its dense object detection capability, enabling it to detect objects at small scales and under heavy occlusion. For hand detection, VarifocalNet outperforms other object detection methods in terms of AP and AP_{75} . In terms of AP_{50} , DINO achieves the best performance.

The confusion matrix for the standard object detection method, Faster R-CNN, is shown in Figure 6. We observe that tools with similar textures and shapes are often misclassified (e.g., scissors and needle holders). Additionally, tools with many varieties of appearances are confused with backgrounds (e.g., forceps, gauze, and retractors).

We compare the hand detection performance of different training data and pre-training data settings using Faster R-CNN in Table 5. Training with our EgoSurgery-Tool dataset significantly outperforms training with the existing hand dataset, EgoHands, which was collected in a daily living setting. Despite the vast quantity of annotated data in EgoHands, models trained solely on EgoHand perform substantially worse compared to those trained with our EgoSurgery-Tool, suggesting a significant domain transfer problem related to the characteristics and representation of

Table 4. Performance of object detection methods on the EgoSurgery-Tool. The best performance is shown in bold.

(a) Surgical tool detection performance.			
Methods	AP	AP_{50}	AP_{75}
Faster R-CNN [14]	37.7	55.8	43.3
RetinaNet [11]	36.2	53.0	39.8
Cascade R-CNN [4]	38.8	55.7	44.6
CenterNet [24]	42.4	60.2	46.8
Sparse R-CNN [18]	37.0	55.1	41.8
VarifocalNet [23]	45.8	63.3	51.1
Deformable-DETR [25]	30.0	46.3	34.0
DDQ [22]	43.2	59.1	48.7
DINO [20]	39.7	56.7	43.5
(b) Hand detection performance.			
Methods	AP	AP_{50}	AP_{75}
Faster R-CNN [14]	55.3	80.4	62.3
RetinaNet [11]	57.1	81.9	62.9
Cascade R-CNN [4]	55.5	80.7	61.4
CenterNet [24]	56.6	78.5	63.3
Sparse R-CNN [18]	55.4	78.7	60.9
VarifocalNet [23]	59.4	82.1	65.3
Deformable-DETR [25]	54.1	78.6	59.2
DDQ [22]	58.3	73.5	60.8
DINO [20]	58.8	80.2	65.6

Table 5. Left: Faster-RCNN hand detection performance comparison between the existing hand detection dataset, EgoHands, and our dataset. Right: Pretrained Faster-RCNN hand detection performance with fine-tuning on our dataset, separated by training order.

Training data	AP	Pre-training dataset	AP
EgoHands	8.9	ImageNet	50.7
Ours	55.3	COCO	55.3
		COCO, EgoHands	52.1

hands in a surgical environment. We also explored the performance of hand detection with different pre-training data. Pre-training with COCO achieves the best performance. Due to the significant domain gap, pre-training with the existing hand detection dataset, EgoHands, degrades performance.

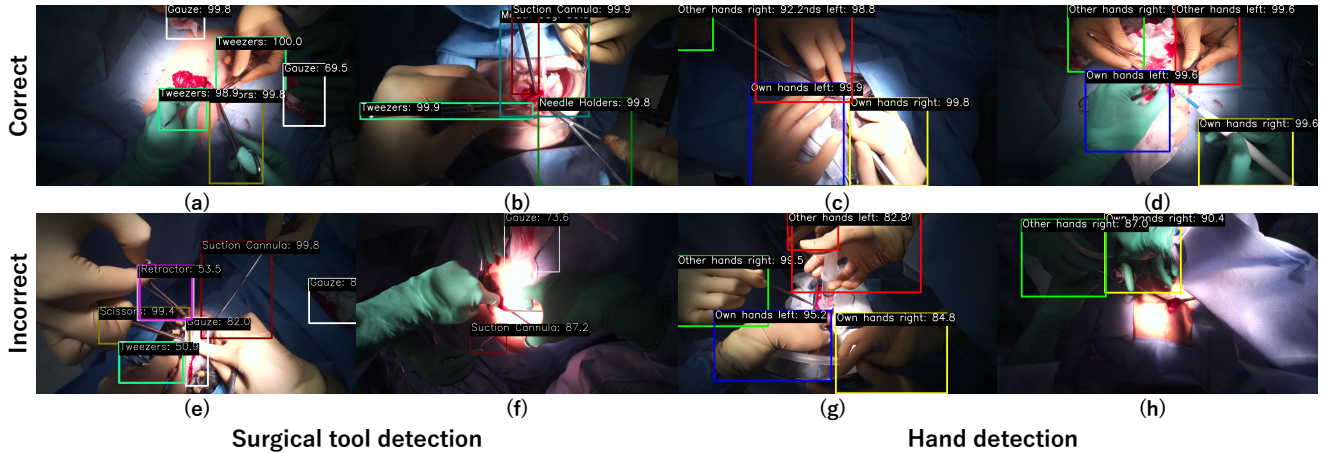


Figure 5. Qualitative results for the object detection challenge. The first column shows correct detections, while the second column shows incorrect cases.

	Bipolar Forceps	Electric Cautery	Forceps	Gauze	Hook	Mouth Gag	Needle Holders	Raspatory	Retractor	Scalpel	Scissors	Skewer	Suction Cannula	Syringe	Tweezers	background
Bipolar Forceps	59%	0%	0%	0%	0%	7%	2%	0%	1%	1%	0%	0%	0%	12%	12%	
Electric Cautery	0%	61%	0%	0%	0%	0%	0%	0%	14%	0%	0%	0%	0%	0%	0%	23%
Forceps	0%	0%	12%	0%	0%	0%	8%	2%	0%	8%	0%	3%	0%	5%	57%	
Gauze	0%	0%	0%	61%	0%	0%	0%	0%	0%	0%	0%	0%	0%	1%	34%	
Hook	0%	0%	0%	0%	30%	0%	0%	4%	2%	2%	3%	10%	4%	13%	25%	
Mouth Gag	0%	0%	0%	0%	0%	67%	0%	0%	0%	0%	0%	0%	0%	0%	0%	1%
Needle Holders	1%	1%	1%	0%	0%	0%	59%	0%	0%	9%	0%	1%	0%	8%	14%	
Raspatory	3%	0%	0%	0%	0%	0%	1%	54%	0%	1%	3%	9%	5%	0%	9%	
Retractor	0%	1%	1%	2%	1%	0%	1%	0%	5%	0%	4%	0%	8%	0%	5%	65%
Scalpel	0%	2%	0%	0%	0%	0%	0%	5%	0%	62%	1%	2%	0%	0%	11%	10%
Scissors	0%	0%	2%	0%	0%	0%	13%	0%	0%	0%	40%	0%	2%	0%	4%	33%
Skewer	0%	0%	0%	2%	0%	0%	17%	0%	0%	0%	66%	5%	0%	0%	0%	7%
Suction Cannula	0%	0%	0%	0%	0%	0%	4%	0%	3%	0%	1%	0%	63%	0%	1%	23%
Syringe	2%	4%	0%	2%	0%	3%	1%	0%	0%	9%	0%	0%	0%	43%	3%	29%
Tweezers	1%	0%	0%	0%	0%	0%	0%	1%	0%	2%	1%	0%	0%	0%	77%	12%
background	0%	2%	4%	38%	1%	0%	14%	0%	2%	1%	6%	0%	10%	0%	14%	0%

Figure 6. Confusion matrix of surgical tool detection model.

3.3. Qualitative results

Figure 5 presents qualitative results for Faster-RCNN using IoU thresholds of 0.5. The model successfully detects surgical tools in (a, b) and hands wearing different colors of surgeons' gloves in (c, d) across a variety of surgery types. Examples of detection failures are shown in (e)-(h). Heavy occlusion (e, h), poor lighting conditions (f), and similar shapes and textures between categories (e, g) cause these incorrect detections.

4. Conclusion

To address the lack of a large-scale dataset in the open surgery domain, we introduce EgoSurgery-Tool, an egocentric open surgery video dataset captured from a camera attached to the surgeon's head, including bounding box annotations for surgical tools and hands. We conducted extensive evaluations of recent object detection methods on this new benchmark dataset. We believe the dense annotations of EgoSurgery-Tool will foster future research in video understanding within the open surgery domain.

ACKNOWLEDGMENT

This work was supported by JSPS KAKENHI Grant Number 22H03617.

References

- [1] Mansoor Ali, Gilberto Ochoa-Ruiz, and Sharib Ali. A semi-supervised Teacher-Student framework for surgical tool detection and localization. *CMBBE*, 2022. 2
- [2] Andrew Zisserman Arpit Mittal and Philip Torr. Hand detection using multiple proposals. In *BMVC*, 2011. 2
- [3] Sven Bambach, Stefan Lee, David J. Crandall, and Chen Yu. Lending A Hand: Detecting Hands and Recognizing Activities in Complex Egocentric Interactions. In *ICCV*, 2015. 2
- [4] Zhaowei Cai and Nuno Vasconcelos. Cascade R-CNN: Delving Into High Quality Object Detection. In *CVPR*, June 2018. 3, 4
- [5] Kai Chen, Jiaqi Wang, Jiangmiao Pang, Yuhang Cao, Yu Xiong, Xiaoxiao Li, Shuyang Sun, Wansen Feng, Ziwei Liu, Jiarui Xu, Zheng Zhang, Dazhi Cheng, Chenchen Zhu, Tianheng Cheng, Qijie Zhao, Buyu Li, Xin Lu, Rui Zhu, Yue Wu, Jifeng Dai, Jingdong Wang, Jianping Shi, Wanli Ouyang, Chen Change Loy, and Dahua Lin. MMDetection: Open

- mmlab detection toolbox and benchmark. *arXiv preprint*, 2019. 3
- [6] Goodman et al. Analyzing Surgical Technique in Diverse Open Surgical Videos With Multitask Machine Learning. *JAMA Surgery*, 2024. 2
- [7] Ryo Fujii, Ryo Hachiuma, Hiroki Kajita, and Hideo Saito. Surgical Tool Detection in Open Surgery Videos. *Applied Sciences*, 2022. 2
- [8] Ryo Fujii, Ryo Hachiuma, and Hideo Saito. Weakly Semi-Supervised Tool Detection in Minimally Invasive Surgery Videos. In *ICASSP*, 2024. 2
- [9] Ryo Fujii, Masashi Hatano, Hideo Saito, and Hiroki Kajita. EgoSurgery-Phase: A Dataset of Surgical Phase Recognition from Egocentric Open Surgery Videos. *arXiv preprint*, 2024. 2
- [10] Amy Jin, Serena Yeung, Jeffrey Jopling, Jonathan Krause, Dan Azagury, Arnold Milstein, and Li Fei-Fei. Tool detection and operative skill assessment in surgical videos using region-based convolutional neural networks. In *WACV*, 2018. 2
- [11] Tsung-Yi Lin, Priya Goyal, Ross Girshick, Kaiming He, and Piotr Dollár. Focal loss for dense object detection. In *ICCV*, 2017. 3, 4
- [12] Tsung-Yi Lin, Michael Maire, Serge Belongie, James Hays, Pietro Perona, Deva Ramanan, Piotr Dollár, and C Lawrence Zitnick. Microsoft coco: Common objects in context. In *ECCV*, 2014. 3
- [13] Ashwin Raju, Heng Wang, and Junzhou Huang. M2cai surgical tool detection challenge report. *University of Texas at Arlington, Tech. Rep.*, 2016. 2
- [14] Shaoqing Ren, Kaiming He, Ross Girshick, and Jian Sun. Faster R-CNN: Towards Real-Time Object Detection with Region Proposal Networks. In *NeurIPS*, 2015. 3, 4
- [15] Duygu Sarikaya, Jason J. Corso, and Khurshid A. Guru. Detection and Localization of Robotic Tools in Robot-Assisted Surgery Videos Using Deep Neural Networks for Region Proposal and Detection. *T-MI*, 2017. 2
- [16] Dandan Shan, Jiaqi Geng, Michelle Shu, and David F. Fouhey. Understanding Human Hands in Contact at Internet Scale. In *CVPR*, 2020. 2
- [17] Pan Shi, Zijian Zhao, Sanyuan Hu, and Faliang Chang. Real-time surgical tool detection in minimally invasive surgery based on attention-guided convolutional neural network. *IEEE Access*, 2020. 2
- [18] Peize Sun, Rufeng Zhang, Yi Jiang, Tao Kong, Chenfeng Xu, Wei Zhan, Masayoshi Tomizuka, Lei Li, Zehuan Yuan, Changhu Wang, and Ping Luo. Sparse R-CNN: End-to-End Object Detection With Learnable Proposals. In *CVPR*, 2021. 3, 4
- [19] Armine Vardazaryan, Didier Mutter, Jacques Marescaux, and Nicolas Padoy. Weakly-supervised learning for tool localization in laparoscopic videos. In *MICCAI*, 2018. 2
- [20] Hao Zhang, Feng Li, Shilong Liu, Lei Zhang, Hang Su, Jun Zhu, Lionel Ni, and Heung-Yeung Shum. DINO: DETR with Improved DeNoising Anchor Boxes for End-to-End Object Detection. In *ICLR*, 2023. 3, 4
- [21] Michael Zhang, Xiaotian Cheng, Daniel Copeland, Arjun Desai, Melody Guan, Gabriel Brat, and Serena Yeung. Using Computer Vision to Automate Hand Detection and Tracking of Surgeon Movements in Videos of Open Surgery. *AMIA*, 2021. 2
- [22] Shilong Zhang, Xinjiang Wang, Jiaqi Wang, Jiangmiao Pang, Chengqi Lyu, Wenwei Zhang, Ping Luo, and Kai Chen. Dense Distinct Query for End-to-End Object Detection. In *CVPR*, 2023. 3, 4
- [23] Zhang, Haoyang and Wang, Ying and Dayoub, Feras and Sünderhauf, Niko. Varifocalnet: An iou-aware dense object detector. In *CVPR*, 2021. 3, 4
- [24] Zhou, Xingyi and Wang, Dequan and Krähenbühl, Philipp. Objects as points. *arXiv preprint*, 2019. 3, 4
- [25] Xizhou Zhu, Weijie Su, Lewei Lu, Bin Li, Xiaogang Wang, and Jifeng Dai. Deformable DETR: Deformable Transformers for End-to-End Object Detection. In *ICLR*, 2021. 3, 4
- [26] Aneeq Zia, Kiran Bhattacharyya, Xi Liu, Max Berniker, Ziheng Wang, Rogerio Nespolo, Satoshi Kondo, Satoshi Kasai, Kousuke Hirasawa, Bo Liu, David Austin, Yiheng Wang, Michal Futrega, Jean-Francois Puget, Zhenqiang Li, Yoichi Sato, Ryo Fujii, Ryo Hachiuma, Mana Masuda, Hideo Saito, An Wang, Mengya Xu, Mobarakol Islam, Long Bai, Winnie Pang, Hongliang Ren, Chinedu Nwoye, Luca Sestini, Nicolas Padoy, Maximilian Nielsen, Samuel Schüttler, Thilo Sentker, Hümeyra Husseini, Ivo Baltruschat, Rüdiger Schmitz, René Werner, Aleksandr Matsun, Mugariya Farooq, Numan Saaed, Jose Renato Restom Viera, Mohammad Yaqub, Neil Getty, Fangfang Xia, Zixuan Zhao, Xiaotian Duan, Xing Yao, Ange Lou, Hao Yang, Jintong Han, Jack Noble, Jie Ying Wu, Tamer Abdalbaki Alshirbaji, Nour Aldeen Jalal, Herag Arabian, Ning Ding, Knut Moeller, Weiliang Chen, Quan He, Muhammad Bilal, Taofeek Akinosho, Adnan Qayyum, Massimo Caputo, Hunaid Vohra, Michael Loizou, Anuoluwapo Ajayi, Ilhem Berrou, Faatihah Niyi-Odomosu, Lena Maier-Hein, Danail Stoyanov, Stefanie Speidel, and Anthony Jacr. Surgical tool classification and localization: results and methods from the MICCAI 2022 SurgToolLoc challenge. *arXiv preprint*, 2023. 2